Inorganic Chemistry
Article
Cite This: Inorg. Chem. 2018, 57, 9873−9879
pubs.acs.org/IC

Observation of Cooperative Electronic Quantum Tunneling: Increasing Accessible Nuclear States in a Molecular Qudit

Eufemio Moreno-Pineda,*[,†] Svetlana Klyatskaya,[†] Ping Du,[†] Marko Damjanović,[†] Gheorghe Taran,[‡] Wolfgang Wernsdorfer,*[,†,‡,§] and Mario Ruben*[,†,∥]

[†]Institute of Nanotechnology, Karlsruhe Institute of Technology, Hermann-von-Helmholtz-Platz 1, D-76344 Eggenstein-Leopoldshafen, Germany

[‡]Physikalisches Institut, Karlsruhe Institute of Technology, D-76131 Karlsruhe, Germany

[§]Institut Néel, CNRS, Université Grenoble Alpes, 25 rue des Martyrs, F-38000 Grenoble, France

[∥]Institut de Physique et Chimie des Matériaux de Strasbourg, CNRS, Université de Strasbourg, 23 rue du Loess, BP 43, F-67034 Strasbourg Cedex 2, France

Supporting Information

ABSTRACT: As an extension of two-level quantum bits (qubits), multilevel systems, so-called qu*d*its, where *d* represents the Hilbert space dimension, have been predicted to reduce the number of iterations in quantum-computation algorithms. This has been tested in the well-known $[TbPc_2]^0$ single-molecule magnet (SMM), which allowed implementation of the Grover algorithm in a single molecular unit. In the quest for molecular systems possessing an increased number of accessible nuclear spin states, we explore herein a dimeric Tb_2-SMM via single-crystal μ-SQUID measurements at sub-Kelvin temperatures. We observe ferromagnetic interactions between the Tb^{III} ions and cooperative quantum tunneling of the electronic spins with spin ground state $|J_z = \pm 6\rangle$. Strong hyperfine coupling with the Tb^{III} nuclear spins leads to a multitude of spin-reversal paths, leading to seven strong hyperfine-driven tunneling steps in the hysteresis loops. Our results show the possibility of reading out the Tb^{III} nuclear spin states via cooperative tunneling of the electronic spins, making the dimeric Tb_2-SMM an excellent nuclear spin qu*d*it candidate with $d = 16$.

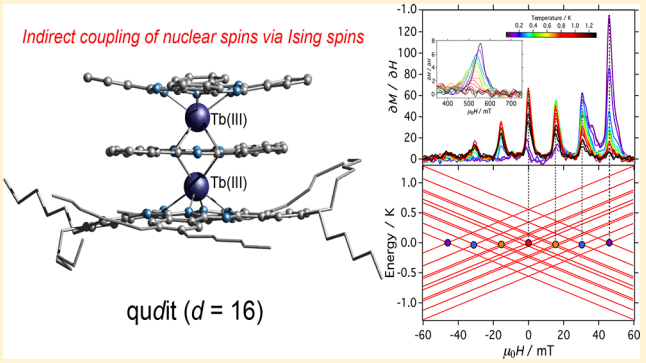

INTRODUCTION

Exploitation of the quantum properties in device applications has boosted numerous studies of molecules exhibiting slow relaxation of magnetization, termed single-molecule magnets (SMMs).[1−6] Moreover, these systems have shown a variety of quantum effects such as the quantum tunneling of magnetization (QTM),[3] Berry phase,[4] quantum oscillations,[5] and entanglement.[6] In addition, SMM systems have also been proposed as parts of quantum computers acting as quantum bits (so-called qubits).[7]

Among the numerous SMMs, the family of terbium(III) bis(phthalocyaninato) ($[TbPc_2]^{0,1\pm}$) complexes has been proposed and established as qubits.[8,9] The electronic properties of $[TbPc_2]^0$ permitted the integration of a single molecule in a transistor circuit, allowing the initialization, manipulation, and read-out of the nuclear spin states.[9] In particular, in the $[TbPc_2]^0$ complex, the Ising-like magnetic anisotropy isolates the ground doublet state $|J_z = \pm 6\rangle$ from excited states, while the hyperfine (hf) interaction couples the electronic spin to the nuclear spin ($|I = {}^3/_2\rangle$) of the $^{159}Tb^{III}$ central ion. Consequently, the nuclear spin states contained in $[TbPc_2]^0$ can be described as an effective two-qubit system, also known as qu*d*it ($d = 4$, representing the dimensions of the qu*d*it).[9−12] The inherent multilevel characteristics, as well as the shielded nature of the nuclear spins against decoherent environmental fluctuations (electronic, magnetic, etc.), have ultimately led to the implementation of Grover's quantum algorithm on a single $[TbPc_2]^0$ molecule.[9d,10]

Two main characteristics allow the use of the $[TbPc_2]^0$ molecule as a qu*d*it: (i) the inherent multilevel properties (qu*d*its where $d > 2$) and (ii) the presence of hf-QTM events. Because of the multiplicity in $[TbPc_2]^0$, entanglement and superposition of multiple states can be achieved in qu*d*its in large dimensions with smaller clusters of processing units,[9,12] while the resonant hf-QTM allows manipulation and read-out of the nuclear spin states via the reversal of the electronic spins.[9d,e]

In this work, we show how the ferromagnetic interaction between the electronic spins in a dinuclear complex, namely,

Received: March 28, 2018
Published: July 31, 2018

DOI: 10.1021/acs.inorgchem.8b00823
Inorg. Chem. 2018, 57, 9873−9879

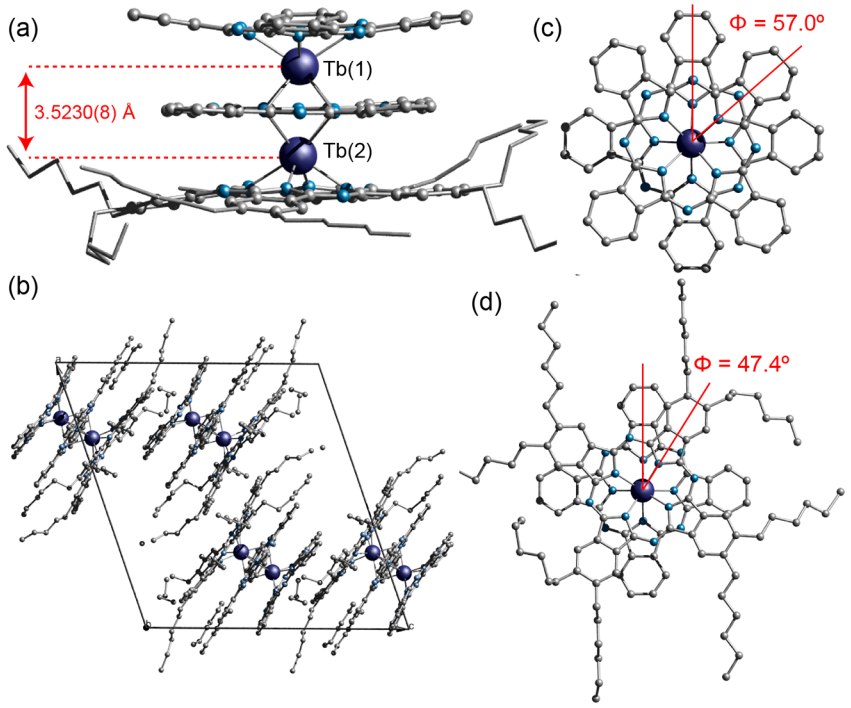

Figure 1. (a) Side view of the crystal structure of **1**. The red double arrow indicates the Tb···Tb intramolecular distance. (b) Representation of the packing diagram showing a quasi-single orientation of the **1** units within the crystal lattice (view along the [010] plane). (c and d) Respective skew angles for the Tb^{III} ion sandwiched between two Pc groups and one Pc and ^{Hx8}Pc groups. Color code: Tb, dark blue; N, cyan; C, gray. H atoms omitted for clarity.

$[Tb_2Pc^{Hx8}Pc_2]$ (**1**), increases the multiplicity of nuclear spin states available for manipulation. Our results show, for the first time (despite a large number of previously reported triple-decker lanthanide complexes),[13] that reversal of the electronic spins occurs via cooperative tunneling (cotunneling) at specific level crossings, induced by the interaction operating between the electronic states of the Tb^{III} ions.

RESULTS AND DISCUSSION

Synthesis and Crystal Structure. The studied SMM, namely, $[Tb_2Pc^{Hx8}Pc_2]$ (**1**, where Pc = phthalocyaninato and ^{Hx8}Pc = 2,3,9,10,16,17,23,24-octahexylphthalocyaninato), was synthesized following a modified reported procedure (see the Supporting Information for details).[14] The complex is extremely robust, allowing its purification via column chromatography. **1** comprises an asymmetric terbium dinuclear complex, composed of two Pc and one ^{Hx8}Pc ligands (Figure 1). The complex crystallizes in the monoclinic $P2_1/c$ space group, with four molecules residing in the unit cell. Two molecules are related by an inversion center, with the other two generated by screw-and-glide-plane symmetries. Coincidentally, both sets of molecules are nearly parallel, with a small tilting angle of 6° between them. At the metal site, each Tb^{III} ion has a distorted-square-antiprism local symmetry: Tb(1) is sandwiched between the two Pc ligands with a continuous shape measure (CShM)[15] value of 1.593, while Tb(2) is sandwiched between one Pc and one ^{Hx8}Pc (a CShM of 2.553; see Table S2). Both Tb^{III} ions possess a more distorted coordination environment than other members of the parent $[TbPc_2]^{0,1-}$ family.[3d] The intramolecular Tb···Tb distance observed in the crystal structure is 3.5230(8) Å, while the shortest intermolecular Tb···Tb distance is 10.8571(7) Å; thus, intermolecular interactions are expectedly small.

Magnetic Description. Magnetic measurements were conducted by employing the neat sample **1** and a magnetically diluted sample, i.e., 1% **1** into 99% $[Y_2Pc^{Hx8}Pc_2]$ ($\mathbf{1}^{dil}$), where intermolecular dipolar fields are strongly reduced. The investigations were conducted in the region of 2 K $\leq T \leq$ 300 K using a commercial SQUID magnetometer. The temperature-dependent magnetic susceptibility $\chi_M T(T)$ of the powder sample **1** exhibits a room temperature value in agreement with the expected value for two non-interacting Tb^{III} ions, i.e., 23.5 $cm^3\ mol^{-1}$ K compared to 23.6 $cm^3\ mol^{-1}$ K (for two Tb^{III} ions with $g_J = {}^3/_2$, where $J = 6$). Upon cooling, $\chi_M T(T)$ stays practically constant up to ca. 16 K, where it sharply increases to 35.3 $cm^3\ mol^{-1}$ K because of ferromagnetic interactions between the Tb^{III} ions, caused probably by a combination of dipolar and exchange interactions (vide infra).[13,14] The same behavior is observed in $\mathbf{1}^{dil}$ (Figures 2 and S3). Likewise, magnetization (M) versus applied field (H) studies between 2 and 5 K (from 0 to 7 T) show that the saturation value for **1** is reached at relatively low fields (ca. 1 T), leading to an $M(H)$ value of 9.2 μ_B at 7 T. Moreover, alternating magnetic susceptibility studies, conducted at zero direct-current (dc) field for both samples **1** and $\mathbf{1}^{dil}$, show a frequency-dependent magnetic behavior characterized by a single relaxation process. **1** can, therefore, be described as an SMM (Figures 2b and S4 and S5).

Single-Crystal Studies. The nuclear spins embodied in the $^{159}Tb^{III}$ metal ions, the small interaction between the ions, and the SMM character make **1** an excellent candidate for investigating hf-QTM. The important question here is whether the observed small ferromagnetic interaction occurring between electronic spins of the Tb^{III} ions allows the coupling of the Tb^{III} nuclear spin, thus increasing the number of accessible nuclear states that could be utilized for testing

DOI: 10.1021/acs.inorgchem.8b00823
Inorg. Chem. 2018, 57, 9873−9879

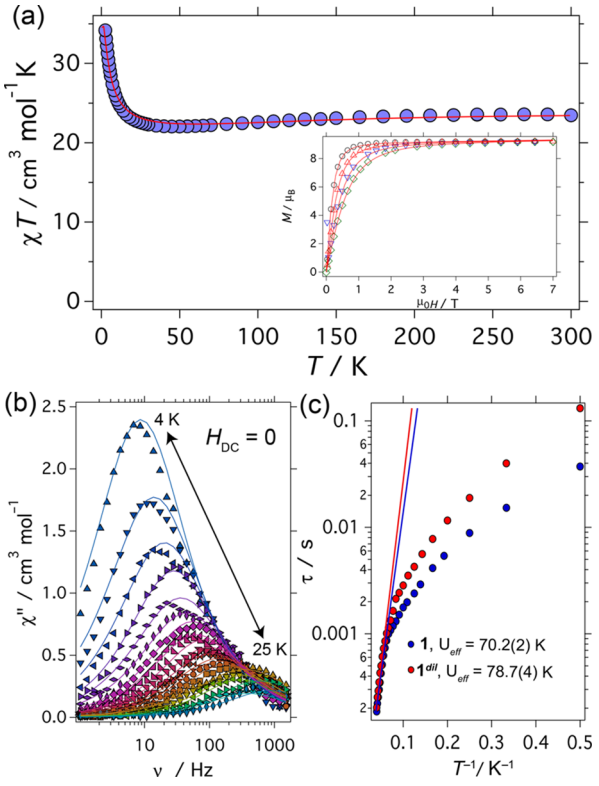

Figure 2. (a) $\chi_M T(T)$ and $M(H)$ (inset) data for compound **1** and simulation (solid lines) using the Hamiltonian (3) and parameters described in the text. (b) $\chi''(\nu)$ experimental data for $\mathbf{1}^{dil}$ with $H_{dc} = 0$ and an oscillating field of 3.5 Oe. Solid lines are fits to a single Debye process. (c) τ versus $1/T$ data for complex **1** (blue ●) and $\mathbf{1}^{dil}$ (red ●) and Arrhenius analysis (solid lines).

quantum algorithms. In order to answer this question, we studied a single crystal of $\mathbf{1}^{dil}$ at sub-Kelvin temperatures with the μ-SQUID technique.[16] Employing the transverse field method, the magnetic field was applied along the mean easy axis of magnetization, which lies close to the [101] crystallographic plane.[17] Figure 3 shows open hysteresis loops at different magnetic-field sweep rates and temperatures (Figures 3 and S6), confirming the SMM behavior. In particular, the hysteresis loops in the vicinity of $\mu_0 H_z = 0$ show a staircase-like structure with seven main transitions occurring at 0, ±15.4, ±30.4 and ±45.7 mT (Figures 3 and 4a,b). Furthermore, two additional broad transitions are observed at ±550 mT (Figures 4b, inset, and S8). This observation of seven transitions is different from but also analogous to the behavior of the parent mononuclear $[TbPc_2]^{1\pm,0}$ complex, which shows only four hf-QTM transitions at ±12 and ±37 mT. These correspond to the avoided level crossings that conserve the nuclear spin of the Tb^{III} ion. The tunnel splittings are a result of the transverse ligand-field interactions, which are caused by the transverse crystal-field terms ($A_4^4\hat{O}_4^4$ and $A_6^4\hat{O}_6^4$) arising from a small distortion of the D_{4d} symmetry of the molecule.[3d] Note that a recently reported fused Pc-bridged Tb dimer, with a relatively long intramolecular Tb···Tb distance of 11.3135(7) Å, exhibits only four hf-QTM transitions,[18] suggesting that the two Tb-containing moieties act as two rather independent SMM units. Furthermore, a mixed heteronuclear Tb^{III}–Dy^{III} dimeric SMM with geometrical parameters almost identical with those found in **1** does show only four hf-QTM transitions.[14b] The lack of additional QTM transitions in the dimeric Tb^{III}–Dy^{III} SMM could be ascribed to the isotopic mixture of nuclear states in the Dy^{III} ions as well as smaller or quenched Tb^{III}···Dy^{III} interactions.

In the following, it will be shown that the electronic states of the Tb^{III} ions of **1** are effectively coupled and the observed multitude of hf-QTM steps can be assigned to a cotunneling of the electronic spin $|J_z = \pm 6\rangle$, while the nuclear spin states are conserved. For this purpose, we choose a ligand-field (lf) Hamiltonian that takes into account the distorted electronic environment of the two Tb^{III} ions in $\mathbf{1}^{dil}$, imposing locally an approximate C_4 symmetry:[3d,20,21]

$$\mathcal{H}^i_{lf} = \alpha A_2^0\hat{O}_2^0 + \beta(A_4^0\hat{O}_4^0 + A_4^4\hat{O}_4^4) + \gamma(A_6^0\hat{O}_6^0 + A_6^4\hat{O}_6^4) \quad (1)$$

where $i = 1$ or 2 refers to each Tb^{III} ion, α, β, and γ are the Stevens coefficients, $\hat{O}_k^q$ are the equivalent Stevens operators, and A_k^q are the ligand-field parameters. In order to account for the effect of the magnetic field and Tb^{III} nuclear spin on the multiplicity of the m_J states, three other terms are included:

$$\mathcal{H}^i_{Tb} = \mathcal{H}^i_{lf} + g_J\mu_0\mu_B\mathbf{J}^i_z\cdot\mathbf{H}_z + A_{hf}\mathbf{I}^i\cdot\mathbf{J}^i_z + P\left[(I^i_z)^2 - \frac{1}{3}(I+1)\mathbf{I}\right] \quad (2)$$

In eq 2, the second term describes the Zeeman interaction and the third and fourth terms describe the hyperfine and quadrupole interactions, respectively, with A_{hf} and P the corresponding parameters. The ligand-field parameters of a closely related molecule have been experimentally determined from NMR and magnetic susceptibility data, where the A_k^q parameters are slightly different for each Tb^{III} site, reflecting the asymmetry of the molecule.[20] Likewise, the A_4^4 and A_6^4 terms in ref 20 are larger than that of the mononuclear $[TbPc_2]^-$ analogues.[3d] Despite the differences of A_k^q compared to the parameters of the archetypal $[TbPc_2]^-$ complex, the ground state for each Tb^{III} ion is well-defined as $|J_z = \pm 6\rangle$. Given that the accurate determination of high-order terms is rather difficult, in our analysis, we solely employed the A_k^q (where $k = 2$ and 4, while $q = 0$) terms reported in ref 20, i.e., $A_2^0 = +289$ cm^{-1} and $A_4^0 = -209$ cm^{-1} for Tb(1) and $A_2^0 = +293$ cm^{-1} and $A_4^0 = -197$ cm^{-1} for Tb(2), while the remaining terms are set to zero. Because of the close proximity of the Tb^{III} ions, i.e., an intramolecular Tb···Tb distance of 3.5230(8) Å (vide supra), both ions are connected by a weak dipolar interaction of the form[13c] $\mathcal{H}_{dip}$ (see section 3 in the Supporting Information for a more detailed description). Thus, the Hamiltonian for $\mathbf{1}^{dil}$ reads

$$\mathcal{H} = -2J_1\cdot\mathcal{H}_{dip}\cdot J_2 + \mathcal{H}^1_{Tb} + \mathcal{H}^2_{Tb} \quad (3)$$

The energy diagram of $\mathbf{1}^{dil}$ can be calculated by the exact diagonalization of the $(2J+1)^2(2I+1)^2(2J+1)^2(2I+1)^2$ Hamiltonian (3). For simplicity, we assume P and A_{hf} for both sites to be equal. Employing A_{hf} and P as parameters, we are able to reproduce the seven QTM events observed in the μ-SQUID data with $P = +0.010$ cm^{-1} and $A_{hf} = +0.0215$ cm^{-1} (Figure 4c) provided that $\mathcal{H}_{dip}$ is larger than the hyperfine coupling (vide infra). We find a P parameter equal to the one found for $[TbPc_2]^-$, while a slightly larger A_{hf} than in the mononuclear case is obtained (cf. $P = +0.010$ cm^{-1} and $A_{hf} = +0.0173$ cm^{-1} for $[TbPc_2]^-$).[3d] Note that the effect of the 6° tilting angle between the two differently oriented molecules in

DOI: 10.1021/acs.inorgchem.8b00823
Inorg. Chem. 2018, 57, 9873–9879

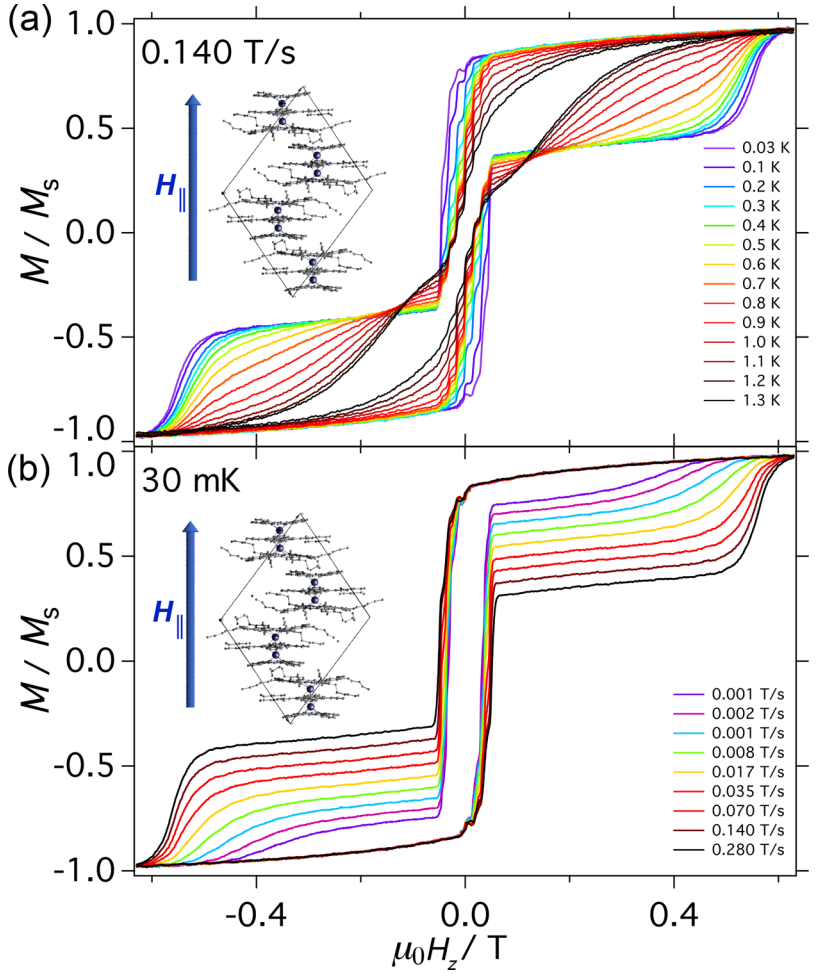

Figure 3. (a) Temperature dependence of magnetization of $\mathbf{1}^{dil}$ at a field sweep rate of 0.140 T/s. (b) Field dependence of magnetization at T = 30 mK. The field was applied parallel to the easy axis of magnetization. Before each field sweep, a waiting time of more than 1000 s at ±1 T was used to thermally equilibrate the nuclear spin system with the thermal bath.

the unit cell causes only a small broadening of each crossing point and does not account for additional QTM events.

Numerical diagonalization of the Hamiltonian given by eq 3 results in 100 level crossings close to zero field and for the $|J_z = \pm 6\rangle|J_z = \pm 6\rangle$ states (Figure 4c). However, out of these, only 10 have large tunnel splittings, leading to a high probability of electronic spin reversal (only seven are observed because, for some crossings, tunneling occurs at the same resonance field). The tunnel splittings are induced by off-diagonal terms in the Hamiltonian, which couple the $|J_z = \pm 6\rangle$ states. In the Tb dimer, both $^{159}Tb^{III}$ ions are coupled by ferromagnetic interaction (vide infra), and the eigenstates can be expressed as $|J_z^a, I_z^a\rangle|J_z^b, I_z^b\rangle$. At very low temperatures, solely the $|-6, I_z^a\rangle|-6, I_z^b\rangle$ states are populated (for positive fields). Before each field sweep, the nuclear spins are thermalized. For this, a waiting time of more than 1000 s at ±1 T was used to thermally equilibrate the nuclear spin system with the thermal bath. The electronic spin reversal occurs at level crossings with large tunnel splittings when the field is swept from a high negative field to a positive one.

The seven events observed in Figure 4b can be rationalized as follows: upon sweeping of the field between ±1 T, tunneling occurs while conserving the nuclear states. At zero field, two tunneling events occur between the $\left|-6, \pm\frac{1}{2}\right\rangle\left|-6, \mp\frac{1}{2}\right\rangle$ and $\left|+6, \pm\frac{1}{2}\right\rangle\left|+6, \mp\frac{1}{2}\right\rangle$ states and also between the $\left|-6, \pm\frac{3}{2}\right\rangle\left|-6, \mp\frac{3}{2}\right\rangle$ and $\left|+6, \pm\frac{3}{2}\right\rangle\left|+6, \mp\frac{3}{2}\right\rangle$ states (red circle in Figure 4c). Two other allowed tunneling events occur at ±15.4 mT, where the reversal occurs via the states $\left|-6, \pm\frac{1}{2}\right\rangle\left|-6, \mp\frac{1}{2}\right\rangle$ to $\left|+6, \pm\frac{1}{2}\right\rangle\left|+6, \mp\frac{1}{2}\right\rangle$ and $\left|-6, \pm\frac{1}{2}\right\rangle\left|-6, \mp\frac{3}{2}\right\rangle$ to $\left|+6, \pm\frac{1}{2}\right\rangle\left|+6, \mp\frac{3}{2}\right\rangle$ (orange circles in Figure 4c). At ±30.4 mT, the reversal is permitted via $\left|-6, \pm\frac{1}{2}\right\rangle\left|-6, \mp\frac{3}{2}\right\rangle$ to $\left|+6, \pm\frac{1}{2}\right\rangle\left|+6, \mp\frac{3}{2}\right\rangle$ (blue circles in Figure 4c), while the last event at ±45.7 mT is ascribed to the electronic spin flip via the $\left|-6, \pm\frac{3}{2}\right\rangle\left|-6, \mp\frac{3}{2}\right\rangle$ to $\left|+6, \pm\frac{3}{2}\right\rangle\left|+6, \mp\frac{3}{2}\right\rangle$ states (purple circles in Figure 4c; see Figure S7 for a detailed description of all states). Therefore, we conclude that simultaneous spin reversals at specific avoided crossings are observed, as long as the nuclear spin states are strictly conserved. As observed in Figure 4b, the cotunnel probability depends not only on the tunnel splittings but also on the thermal population of the levels, yielding a strong temperature dependence of the step height of each transition.

Additionally, at $\mu_0 H_z$ = ±550 mT, two broader transitions are observed (inset in Figure 4b), which are in agreement with

DOI: 10.1021/acs.inorgchem.8b00823
Inorg. Chem. 2018, 57, 9873−9879

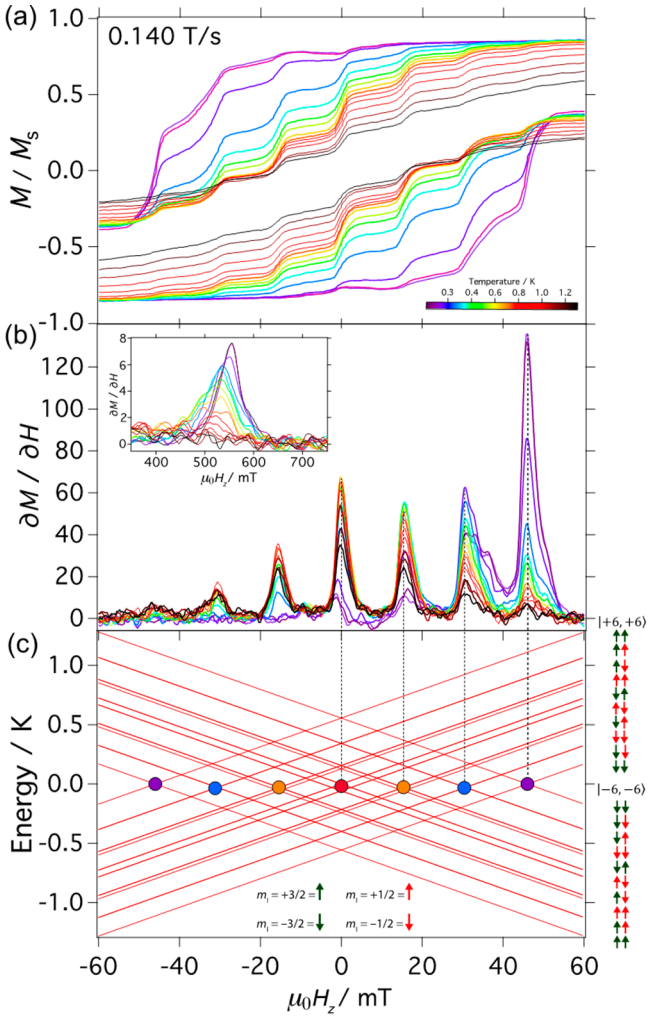

Figure 4. (a) Zoom of the hysteresis loops of Figure 3a recorded between ±1 T with a field sweep of 0.140 T/s at several temperatures, showing a staircase-like structure. (b) First field derivative for a field sweep from −1 to +1 T of the data in part a. (c) Simulated Zeeman diagram with the field parallel to the easy axes, employing eq 3 and A_k^q (where k = 2 and 4, while q = 0) described in the text. hf-QTM is ascribed to cotunneling of the electronic spins, that is, transitions between $|-6, I_z^a\rangle|-6, I_z^b\rangle \leftrightarrow |+6, I_z^a\rangle|+6, I_z^b\rangle$. The arrows to the rightmost side are the pictorial representation of the nuclear spins for every m_I state (see Figure S7 for a detailed description of all states).

a ferromagnetic interaction between the Tb^{III} ions, where single spin flips occur between the electronic ground states, i.e., $|\pm J_z^a, I_z^a\rangle|\mp J_z^b, I_z^b\rangle \leftrightarrow |\pm J_z^a, I_z^a\rangle|\pm J_z^b, I_z^b\rangle$ or $|\mp J_z^a, I_z^a\rangle|\pm J_z^b, I_z^b\rangle \leftrightarrow |\mp J_z^a, I_z^a\rangle|\mp J_z^b, I_z^b\rangle$ (see Figure S8).[13c] The hyperfine structure is not experimentally resolved probably because of small distributions of ligand-field parameters and misalignment. As can be seen in Figure S8, these transitions at $\mu_0 H_z = \pm 550$ mT cannot be reproduced by employing a purely dipolar coupling between the Ising $|J_z = \pm 6\rangle$ states, which places the first excited state at +3.21 cm^{-1} from the ground state [calculated for a Tb···Tb distance of 3.5230(8) Å using a point-dipole approximation]. Experimentally, the first excited state lies at about +4.6 cm^{-1}, which is larger than the calculated dipolar value; therefore, it is possible that, in addition, a small contribution of exchange interaction is present. To assess this possibility, we add an isotropic Heisenberg interaction (J_{ex}) to the dipolar matrix. The Hamiltonian has the following form:

$$\mathcal{H} = -2J_1 \cdot (\mathcal{H}_{dip} + J_{ex}) \cdot J_2 + \mathcal{H}^1_{Tb} + \mathcal{H}^2_{Tb} \quad (4)$$

The simulations were adjusted so that the crossing point between the ground state and first excited state observed through μ-SQUID data at ±500 mT is reproduced. Employing eq 4, we are able to reproduce the crossing point between the first excited state and ground state with J_{ex} = +0.0097 cm^{-1}. Note that solely from the magnetic data it is impossible to accurately assess the possibility of exchange interactions occurring in **1** given that both $\mathcal{H}_{dip}$ and $\mathcal{H}_{dip} + J_{ex}$ equally reproduce the data. Our results show that the possibility of exchange interactions occurring between the Tb^{III} ions is highly probable and requires further studies.

CONCLUSIONS

Hf-driven QTM has been previously observed in several lanthanide complexes;[3d,19] however, what makes **1** really unique is the collective behavior triggered by the small interaction between the two Tb^{III} ions. This interaction leads to a coupling of the nuclear spins of the two $^{159}Tb^{III}$ metal ions, not just causing hf-QTM occurrences, as observed in $[TbPc_2]^-$, but additionally increasing the multiplicity of the nuclear spin states and, as a consequence, allowing hf-QTM at additional resonance field positions. Moreover, the results reported here differ from those of exchange bias QTM, where the resonance fields are shifted as a result of exchange with adjacent nuclei.[3]

In conclusion, the resonant QTM has been investigated in a dimeric Tb^{III}-based SMM via μ-SQUID measurements, allowing determination of the hyperfine and quadrupolar parameters. The hf-QTM events are ascribed to the simultaneous reversal (cotunneling) of the electronic spin, while the nuclear spins are conserved. As in the $[TbPc_2]^{1\pm,0}$ case, the QTM transitions corresponding to each nuclear spin state could be used to read out the nuclear spins in **1** in a qu*d*it scheme as an enlarged quantum register. Note that in the archetypal $[TbPc_2]^{1\pm,0}$, just four states are accessible (corresponding to the $m_I = \pm^3/_2$ and $\pm^1/_2$ states),[9] limiting the applicability of multilevel quantum algorithms. However, in **1**, the observation of an enlarged multiplicity of states by cooperative electronic coupling would open a general avenue to the creation of larger quantum directories, thus allowing the realization of a molecular spin qu*d*it with a exploitable dimension of d = 16 [with $d = (2I + 1)^n$, where n = 2 and $I = {}^3/_2$].[10]

ASSOCIATED CONTENT

Supporting Information

The Supporting Information is available free of charge on the ACS Publications website at DOI: 10.1021/acs.inorgchem.8b00823.

Further synthetic details and structural and magnetic plots (PDF)

Accession Codes

CCDC 1567148−1567149 contain the supplementary crystallographic data for this paper. These data can be obtained free of charge via www.ccdc.cam.ac.uk/data_request/cif, or by emailing data_request@ccdc.cam.ac.uk, or by contacting The Cambridge Crystallographic Data Centre, 12 Union Road, Cambridge CB2 1EZ, UK; fax: +44 1223 336033.

DOI: 10.1021/acs.inorgchem.8b00823
Inorg. Chem. 2018, 57, 9873−9879

AUTHOR INFORMATION

Corresponding Authors

*E-mail: eufemio.pineda@kit.edu.
*E-mail: wolfgang.wernsdorfer@kit.edu.
*E-mail: mario.ruben@kit.edu.

ORCID

Eufemio Moreno-Pineda: 0000-0002-9643-0341
Wolfgang Wernsdorfer: 0000-0003-4602-5257
Mario Ruben: 0000-0002-7718-7016

Notes

The authors declare no competing financial interest.
On occasion of the 60th anniversary of Prof. Kim Dunbar.

ACKNOWLEDGMENTS

We acknowledge the DFG-TR 88 "3Met" (Project A8) and the Karlsruhe Nano Micro Facility (www.kit.edu/knmf) for the provision of access to instruments at their laboratories. W.W. thanks the A. van Humboldt Foundation and the ERC for Grant MoQuOS 741276.

REFERENCES

(1) Gatteschi, D.; Sessoli, R.; Villain, J. *Molecular nanomagnets*; Oxford University Press: Oxford, U.K., 2006.

(2) (a) Sanvito, S. Molecular spintronics. *Chem. Soc. Rev.* **2011**, *40*, 3336. (b) Bogani, L.; Wernsdorfer, W. Molecular spintronics using single-molecule magnets. *Nat. Mater.* **2008**, *7*, 179−186.

(3) (a) Thomas, L.; Lionti, F.; Ballou, R.; Gatteschi, D.; Sessoli, R.; Barbara, B. Macroscopic quantum tunnelling of magnetization in a single crystal of nanomagnets. *Nature* **1996**, *383*, 145−147. (b) Gatteschi, D.; Sessoli, R. Quantum tunneling of magnetization and related phenomena in molecular materials. *Angew. Chem., Int. Ed.* **2003**, *42*, 268−297. (c) Wernsdorfer, W.; Aliaga-Alcalde, N.; Hendrickson, D. N.; Christou, G. Exchange-biased quantum tunnelling in a supramolecular dimer of single-molecule magnets. *Nature* **2002**, *416*, 406−409. (d) Ishikawa, N.; Sugita, M.; Wernsdorfer, W. Quantum Tunneling of Magnetization in Lanthanide Single-Molecule Magnets: Bis(phthalocyaninato)terbium and Bis(phthalocyaninato)dysprosium Anions. *Angew. Chem., Int. Ed.* **2005**, *44*, 2931−2935.

(4) (a) Burzurí, E.; Luis, F.; Montero, O.; Barbara, B.; Ballou, R.; Maegawa, S. Quantum Interference Oscillations of the Superparamagnetic Blocking in an Fe_8 Molecular Nanomagnet. *Phys. Rev. Lett.* **2013**, *111*, 057201. (b) Wernsdorfer, W.; Sessoli, R. Quantum Phase Interference and Parity Effects in Magnetic Molecular Clusters. *Science* **1999**, *284*, 133−135.

(5) Carretta, S.; Santini, P.; Amoretti, G.; Guidi, T.; Copley, J. R. D.; Qiu, Y.; Caciuffo, R.; Timco, G. A.; Winpenny, R. E. P. Quantum Oscillations of the Total Spin in a Heterometallic Antiferromagnetic Ring: Evidence from Neutron Spectroscopy. *Phys. Rev. Lett.* **2007**, *98*, 167401.

(6) (a) Candini, A.; Lorusso, G.; Troiani, F.; Ghirri, A.; Carretta, S.; Santini, P.; Amoretti, G.; Muryn, C.; Tuna, F.; Timco, G.; McInnes, E. J. L.; Winpenny, R. E. P.; Wernsdorfer, W.; Affronte, M. Entanglement in Supramolecular Spin Systems of Two Weakly Coupled Antiferromagnetic Rings (Purple-Cr_7Ni). *Phys. Rev. Lett.* **2010**, *104*, 037203. (b) Garlatti, E.; Guidi, T.; Ansbro, S.; Santini, P.; Amoretti, G.; Ollivier, J.; Mutka, H.; Timco, G.; Vitorica-Yrezabal, I. J.; Whitehead, G. F. S.; Winpenny, R. E. P.; Carretta, S. Portraying entanglement between molecular qubits with four-dimensional inelastic neutron scattering. *Nat. Commun.* **2017**, *8*, 14543.

(7) Troiani, F.; Affronte, M. Molecular spins for quantum information technologies. *Chem. Soc. Rev.* **2011**, *40*, 3119. (b) Lehmann, J.; Gaita-Ariño, A.; Coronado, E.; Loss, D. Molecular spintronics and quantum computing. *J. Mater. Chem.* **2009**, *19*, 1672−1677.

(8) Ishikawa, N.; Sugita, M.; Ishikawa, T.; Koshihara, S.-Y.; Kaizu, Y. Lanthanide Double-Decker Complexes Functioning as Magnets at the Single-Molecular Level. *J. Am. Chem. Soc.* **2003**, *125*, 8694−8695.

(9) (a) Vincent, R.; Klyatskaya, S.; Ruben, M.; Wernsdorfer, W.; Balestro, F. Electronic read-out of a single nuclear spin using a molecular spin transistor. *Nature* **2012**, *488*, 357−360. (b) Thiele, S.; Balestro, F.; Ballou, R.; Klyatskaya, S.; Ruben, M.; Wernsdorfer, W. Electrically driven nuclear spin resonance in single-molecule magnets. *Science* **2014**, *344*, 1135−1138. (c) Godfrin, C.; Thiele, S.; Ferhat, A.; Klyatskaya, S.; Ruben, M.; Wernsdorfer, W.; Balestro, F. Electrical Read-Out of a Single Spin Using an Exchange-Coupled Quantum Dot. *ACS Nano* **2017**, *11*, 3984−3989. (d) Godfrin, C.; Ferhat, A.; Ballou, R.; Klyatskaya, S.; Ruben, M.; Wernsdorfer, W.; Balestro, F. Operating Quantum States in Single Magnetic Molecules: Implementation of Grover's Quantum Algorithm. *Phys. Rev. Lett.* **2017**, *119*, 187702. (e) Moreno-Pineda, E.; Godfrin, C.; Balestro, F.; Wernsdorfer, W.; Ruben, M. Molecular spin qudits for quantum algorithms. *Chem. Soc. Rev.* **2018**, *47*, 501−513.

(10) Morello, A. Quantum search on a single-atom qudit. *Nat. Nanotechnol.* **2018**, *13*, 9−10.

(11) (a) Jenkins, M. D.; Duan, Y.; Diosdado, B.; García-Ripoll, J. J.; Gaita-Ariño, A.; Giménez-Saiz, C.; Alonso, P. J.; Coronado, E.; Luis, F. Coherent manipulation of three-qubit states in a molecular single-ion magnet. *Phys. Rev. B: Condens. Matter Mater. Phys.* **2017**, *95*, 064423. (b) Martínez-Pérez, M. J.; Cardona-Serra, S.; Schlegel, C.; Moro, F.; Alonso, P. J.; Prima-García, H.; Clemente-Juan, J. M.; Evangelisti, M.; Gaita-Ariño, A.; Sesé, J.; van Slageren, J.; Coronado, E.; Luis, F. Gd-Based Single-Ion Magnets with Tunable Magnetic Anisotropy: Molecular Design of Spin Qubits. *Phys. Rev. Lett.* **2012**, *108*, 247213.

(12) (a) O'Leary, D. P.; Brennen, G. K.; Bullock, S. S. Parallelism for quantum computation with qudits. *Phys. Rev. A: At., Mol., Opt. Phys.* **2006**, *74*, 032334. (b) Smith, A.; Anderson, B. E.; Sosa-Martinez, H.; Riofrío, C. A.; Deutsch, I. H.; Jessen, P. S. Quantum Control in the Cs $^6S_{1/2}$ Ground Manifold Using Radio-Frequency and Microwave Magnetic Fields. *Phys. Rev. Lett.* **2013**, *111*, 170502. (c) Man'ko, M. A.; Man'ko, V. I. Entanglement and other quantum correlations of a single qudit state. *Int. J. Quantum Inform.* **2014**, *12*, 1560006.

(13) (a) Katoh, K.; Breedlove, B. K.; Yamashita, M. Symmetry of octa-coordination environment has a substantial influence on dinuclear Tb^{III} triple- decker single-molecule magnets. *Chem. Sci.* **2016**, *7*, 4329−4340. (b) Sakaue, S.; Fuyuhiro, A.; Fukuda, T.; Ishikawa, N. Dinuclear single-molecule magnets with porphyrin−phthalocyanine mixed triple-decker ligand systems giving SAP and SP coordination polyhedral. *Chem. Commun.* **2012**, *48*, 5337−5339. (c) Fukuda, T.; Matsumura, K.; Ishikawa, N. Influence of Intramolecular f-f Interactions on Nuclear Spin Driven Quantum Tunneling of Magnetizations in Quadruple-Decker Phthalocyanine Complexes Containing Two Terbium or Dysprosium Magnetic Centers. *J. Phys. Chem. A* **2013**, *117*, 10447−10454. (d) Horii, Y.; Katoh, K.; Yasuda, N.; Breedlove, B. K.; Yamashita, M. Effects of f−f Interactions on the Single-Molecule Magnet Properties of Terbium(III)−Phthalocyaninato Quintuple-Decker Complexes. *Inorg. Chem.* **2015**, *54*, 3297−3305. (e) Katoh, K.; Horii, Y.; Yasuda, N.; Wernsdorfer, W.; Toriumi, K.; Breedlove, B. K.; Yamashita, M. Multiple-decker phthalocyaninato dinuclear lanthanoid(III) single-molecule magnets with dual-magnetic relaxation processes. *Dalton Trans.* **2012**, *41*, 13582−13600. (f) Katoh, K.; Komeda, T.; Yamashita, M. The Frontier of Molecular Spintronics Based on Multiple-Decker Phthalocyaninato Tb^{III} Single-Molecule Magnets. *Chem. Rec.* **2016**, *16*, 987−1016.

(14) (a) Klyatskaya, S.; Eichhöfer, A.; Wernsdorfer, W. *J.* X-ray Crystallographic Analysis of a Tailor-Made Bis(phthalocyaninato))-Tb^{III} Single-Molecule Magnet as a Fundamental Unit for Supramolecular Spintronic Devices. *Eur. J. Inorg. Chem.* **2014**, *2014*, 4179−4185. (b) Lan, Y.; Klyatskaya, S.; Ruben, M.; Fuhr, O.; Wernsdorfer, W.; Candini, A.; Corradini, V.; Lodi Rizzini, A.; del Pennino, U.; Troiani, F.; Joly, L.; Klar, D.; Wende, H.; Affronte, M. Magnetic interplay between two different lanthanides in a tris-phthalocyaninato

DOI: 10.1021/acs.inorgchem.8b00823
Inorg. Chem. 2018, 57, 9873−9879

complex: a viable synthetic route and detailed investigation in the bulk and on the surface. *J. Mater. Chem. C* **2015**, *3*, 9794−9801.
(15) Alvarez, S.; Alemany, P.; Casanova, D.; Cirera, J.; Llunell, M.; Avnir, D. Shape maps and polyhedral interconversion paths in transition metal chemistry. *Coord. Chem. Rev.* **2005**, *249*, 1693−1708.
(16) Wernsdorfer, W.; Ohm, T.; Sangregorio, C.; Sessoli, R.; Mailly, D.; Paulsen, C. Observation of the Distribution of Molecular Spin States by Resonant Quantum Tunneling of the Magnetization. *Phys. Rev. Lett.* **1999**, *82*, 3903.
(17) Wernsdorfer, W. From micro- to nano-SQUIDs: applications to nanomagnetism. Supercond. *Supercond. Sci. Technol.* **2009**, *22*, 064013.
(18) Morita, T.; Damjanovic, M.; Katoh, K.; Kitagawa, Y.; Yasuda, N.; Lan, Y.; Wernsdorfer, W.; Breedlove, B. K.; Enders, M.; Yamashita, M. Comparison of the Magnetic Anisotropy and Spin Relaxation Phenomenon of Dinuclear Terbium(III) Phthalocyaninato Single-Molecule Magnets Using the Geometric Spin Arrangement. *J. Am. Chem. Soc.* **2018**, *140*, 2995−3007.
(19) (a) Moreno-Pineda, E.; Damjanović, M.; Fuhr, O.; Wernsdorfer, W.; Ruben, M. Nuclear Spin Isomers: Engineering a $Et_4N[DyPc_2]$ Spin Qudit. *Angew. Chem., Int. Ed.* **2017**, *56*, 9915−9919. (b) Chen, Y.-C.; Liu, J.-L.; Wernsdorfer, W.; Liu, D.; Chibotaru, L. F.; Chen, X.- M.; Tong, M.-L. Hyperfine-Interaction-Driven Suppression of Quantum Tunneling at Zero Field in a Holmium(III) Single-Ion Magnet. *Angew. Chem., Int. Ed.* **2017**, *56*, 4996−5000. (c) Ishikawa, N.; Sugita, M.; Wernsdorfer, W. *J. Am. Chem. Soc.* **2005**, *127*, 3650−3651.
(20) (a) Ishikawa, N.; Iino, T.; Kaizu, Y. Interaction between f-Electronic Systems in Dinuclear Lanthanide Complexes with Phthalocyanines. *J. Am. Chem. Soc.* **2002**, *124*, 11440−11447. (b) Ishikawa, N.; Otsuka, S.; Kaizu, Y. The Effect of the f−f Interaction on the Dynamic Magnetism of a Coupled $4f^8$ System in a Dinuclear Terbium Complex with Phthalocyanines. *Angew. Chem., Int. Ed.* **2005**, *44*, 731−733.
(21) Ungur, L.; Chibotaru, L. F. Ab Initio Crystal Field for Lanthanides. *Chem. - Eur. J.* **2017**, *23*, 3708−3718.

DOI: 10.1021/acs.inorgchem.8b00823
Inorg. Chem. 2018, 57, 9873−9879